John von Neumann Institute for Computing

Polyelectrolyte Brushes: A Molecular Dynamics Study

Christian Seidel

published in

NIC Symposium 2001, Proceedings,
Horst Rollnik, Dietrich Wolf (Editor),
John von Neumann Institute for Computing, Jülich,
NIC Series, Vol. **9**, ISBN 3-00-009055-X, pp. 397-405, 2002.

http://www.fz-juelich.de/nic-series/volume9

Polyelectrolyte Brushes: A Molecular Dynamics Study

Christian Seidel

Max-Planck-Institut für Kolloid- und Grenzflächenforschung
14424 Potsdam, Germany
E-mail: seidel@mpikg-golm.mpg.de

We use molecular dynamics simulations to study polyelectrolytes end-grafted to a surface. The simulation model includes counterions explicitly and treats the full Coulomb interaction. As a main result, we find a novel collapsed brush phase. Its nature can be understood by an extended scaling theory. In the collapsed phase, the height of the brush results from a competition between steric repulsion and attraction due to electrostatic correlations. As a result, the monomer density inside the brush becomes independent of grafting density and chain length.

1 Introduction

Polyelectrolytes, i.e., polymers being equipped with ionizable groups, have received a great deal of attention in recent years. In contrast to uncharged polymers, polyelectrolytes are soluble in water. This particular feature makes them environmentally friendly and in many cases the corresponding applications are cost effective. Anchoring polymer chains by one end sufficiently dense to a solid/liquid or air/liquid interface they form a so-called polymer brush, in which the chains are enforced to take a stretched conformation. A schematic representation of a uncharged polymer brush is shown in Fig. 1 (left-hand part). Polyelectrolyte brushes are interesting from the point of view of fundamental as well as

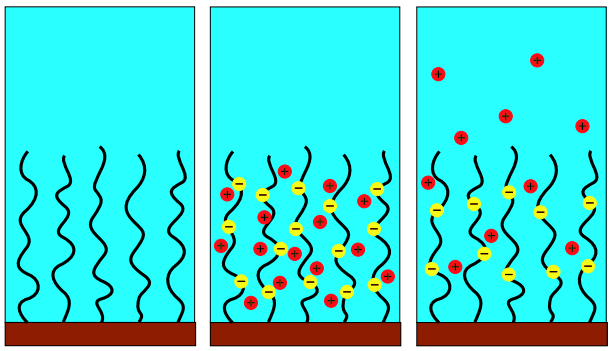

Figure 1. Schematic picture of polymer brushes. Left-hand side: made of uncharged polymers, middle: polyelectrolyte brush at strong charging, left-hand side: polyelectrolyte brush at weak charging.

of applied research. Already for some decades polymer brushes are known as an efficient means for preventing colloids from flocculation[1]. Brushes made of charged chains have the particular advantage that the stabilization arises both from steric and electrostatic effects. In addition, a surface coated with polyelectrolytes is expected to be less sensitive

to the salinity of the surrounding medium than a bare charged surface because a strongly charged brush is able to trap its own counterions and thus generates a layer of large effective ion strength (see Fig. 1, middle part). However, in the weak-charging limit (see Fig. 1, right-hand side) counterions become free to leave the brush and the properties of the polyelectrolyte brush can be drastically changed[2].
Both in experiment and in theoretical work, polyelectrolyte brushes are an interesting subject with many unresolved problems. In this situation, simulations are a promising tool to validate theoretical models and to probe quantities and regimes which are not easily observable experimentally. However, simulations of polyelectrolytes itself remain still challenging despite a strong effort in recent years. The correct treatment of the long-range Coulomb interaction in a periodic system requires special methods which are computational expensive. This task is even more demanding in a slab geometry with spatial periodicity in two directions only which is the case for anchored chain. Under such boundary conditions, a straightforward application of most of the methods known for treating long-range interactions in three-dimensional periodic systems, as e.g. the so-called Ewald sum, is not possible.
In this contribution we report the results of extensive simulation studies on fully charged and on partially charged polyelectrolyte brushes. The paper is organized as follows. In Sec. 2 we shortly review the polyelectrolyte model and the simulation technique. The simulation results are discussed in Sec. 3. In Sec. 4 we compare simulation results with predictions of an extended scaling theory. Conclusions are given in Sec. 5

2 Model and Method

We use a bead-spring model where the polyelectrolytes are composed of charged monomers (for partially charged polyelectrolytes, also uncharged species) which are connected by nonlinear springs and end-grafted to an uncharged surface. The counterions are

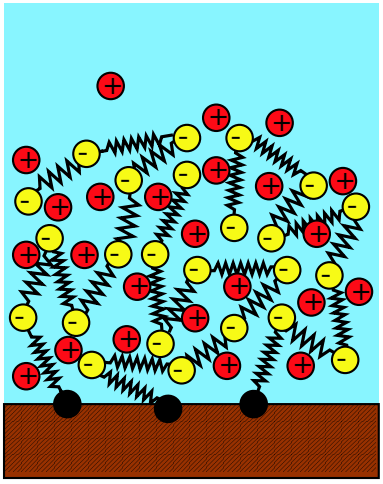

Figure 2. Schematic picture of the simulation model.

free charged particles and there is no additional salt in the system. The solvent (water) is replaced by a dielectric background and a heat bath. A schematic picture of the simulation model is show in Fig. 2. The total potential of the system has four contributions:

$$U = U_{\mathrm{bond}} + U_{\mathrm{LJ}} + U_{\mathrm{wall}} + U_{\mathrm{Coul}}. \tag{1}$$

Besides the bond potential U_{bond} we have a purely repulsive Lennard-Jones term U_{LJ} which models the situation of a polymer in a good solvent. All particles except the fixed anchors interact repulsively with the surface. For this purpose, we use a short-ranged wall potential U_{wall}, which prevents the particles from crossing the surface. The last term in Eq. (1) stands for the Coulomb interaction between all charged particles

$$U_{\mathrm{Coul}} = \lambda_B \, k_B T \sum_{n_x=-\infty}^{\infty} \sum_{n_y=-\infty}^{\infty} \sum_{i=1}^{N_{tot}-1} \sum_{j=i+1}^{N_{tot}} \frac{q_i q_j}{|\mathbf{r}_{ij} + n_x L \mathbf{e}_x + n_y L \mathbf{e}_y|}, \tag{2}$$

where $\lambda_B = e^2/(4\pi\varepsilon_0 \varepsilon k_B T)$ is the Bjerrum length with ε_0 and ε being the vacuum permittivity and the dielectric constant of the solvent, respectively. q_i is the charge of particle i in units of the elementary charge e. $\mathbf{e}_x$ and $\mathbf{e}_y$ are unit vectors in x- and y-direction, respectively, and the indices n_x and n_y run over the periodic images of the simulation box. N_{tot} is the total number of charges, and L is the planar box length. A major task in any simulation of charged systems is to transform conditionally convergent sums like that in Eq. (2) into rapidly convergent series. We use an approach proposed by Lekner and Sperb[3], which allows the transformation of Eq. (2) into an expansion in terms of Bessel functions or Hurwitz zeta functions. Due to the asymptotic behavior of these functions one obtains alternative expressions which are rapidly convergent either at large or small arguments.
We use stochastic molecular dynamics[4,5] to study the system in equilibrium. The equation of motion for particle i at position $\mathbf{r}_i(t)$ is the Langevin equation,

$$m \frac{d^2 \mathbf{r}_i}{dt^2} = -\nabla_i U - m\Gamma \, \frac{d\mathbf{r}_i}{dt} + \mathbf{W}_i(t), \tag{3}$$

where all particles carry the same mass m, and Γ is a friction constant which couples the particles to a heat bath. U is the potential energy defined in Eq. (1). The system is held at thermal equilibrium by a Gaussian random force $\mathbf{W}_i(t)$,

$$\langle \mathbf{W}_i(t) \rangle = 0, \qquad \langle \mathbf{W}_i(t) \cdot \mathbf{W}_j(t') \rangle = 6 m k_{\mathrm{B}} T \Gamma \, \delta_{ij} \delta(t - t'), \tag{4}$$

where the coupling to Γ is a consequence of the fluctuation-dissipation relation. Eq. 3 is integrated using the velocity-Verlet algorithm[5]. The molecular dynamics code was parallelized using a self-scheduling (master-slave) algorithm[6] for the force loop. Upon testing the parallel code for different processor numbers n on a Cray T3E, we found that for our strongly charged systems the efficiency is optimal in the range of $n = 32$ to $n = 64$ processors, where an efficiency of over 90% is reached. Lower numbers of processors lead to a loss in efficiency due to the idle master processor, while large processor numbers are less efficient because communication time becomes a dominant contribution.

3 Simulation Results and Discussion

The molecular dynamics code used in this study allows the investigation of polyelectrolyte brushes in a large parameter range. The contour lengths of the coarse-grained chains mod-

elled in the simulation correspond to about 20 nm - 50 nm which is comparable to experiments on polyelectrolyte brushes at the air/water interface[7]. The grafting densities studied correspond to a surface area per chain between 600 Å^2 and 3000 Å^2, values being typical for experimental systems.

3.1 Completely Charged Chains

In Fig. 3 the dependence of the average brush height on anchoring density is shown for two different Bjerrum lengths (λ_B equal to 0.7 σ and 0.1 σ, with σ being the Lennard-Jones diameter). Note that the average bond length b is about 1.0 σ. Thus, for both Bjerrum lengths, the Manning parameter holds $\xi = \lambda_B/b < 1$. Thus, one would not expect strong counterion-condensation effects, at least for a fully stretched chain at infinite dilution. However, as we will see below, the situation can be quite different in the case of a strongly charged brush.

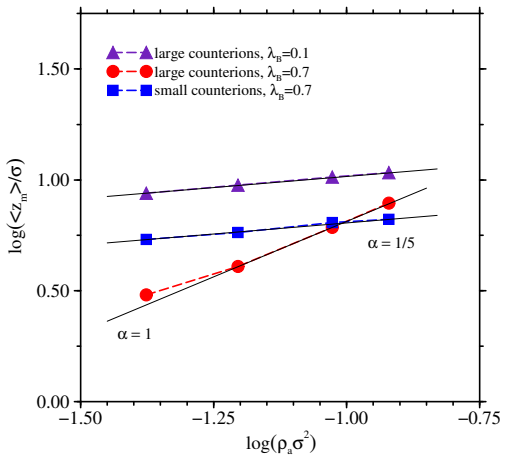

Figure 3. Average brush height versus anchoring density for different interaction strength. Large ci's: $\sigma_{ci} = \sigma_m$, small ci's: $\sigma_{ci} = 0.01\,\sigma_m$. The thin solid lines correspond to power laws with two different exponents α.

For a moderate Bjerrum length $\lambda_B = 0.7\sigma$ (hereafter called strong coupling) we find a linear scaling law $< z_m > \sim \rho_a{}^8$, which is consistent with a constant particle density inside the brush. Our observation of such a collapsed phase disagrees with the accepted scaling law for a charged brush in the so-called osmotic regime which predicts a brush height, independent of grafting density[2]. We believe that this disagreement is caused by the assumption that in the osmotic regime the counterions inside the brush form an ideal gas. Indeed, analyzing the counterion-polyelectrolyte distribution function shown in Fig. 4, it is evident, that strong correlations are present. Note that the scaling law, we observe, is the same as that known for uncharged brushes in a poor solvent. On the other hand, recently it has been shown that counterion correlation (condensed counterions) gives rise to an effective interaction which can change the solvent quality from good to poor[9]. Thus,

strongly charged polyelectrolyte brushes can be considered as a new example of systems where counterion-induced attractions can play an important role. This is a more general topic which received recently a lot of attention in theory and simulations. A more precise understanding of the nature of the collapsed phase we will discuss in Sec. 4.

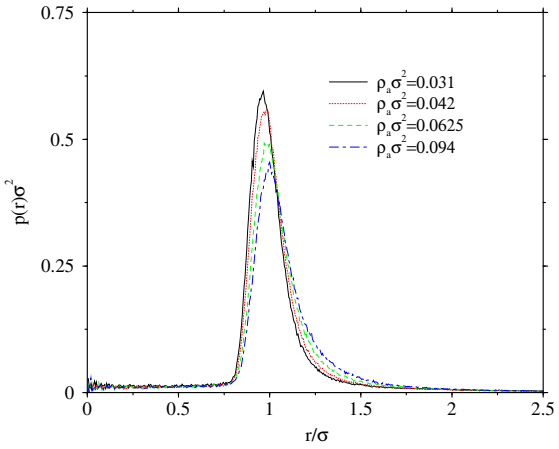

Figure 4. Counterion-polyelectrolyte distribution function at $\lambda_B = 0.7\sigma$ and $\sigma_{ci} = \sigma_m = \sigma$. r is the separation between polyelectrolyte bond and counterion.

For weak Coulomb coupling, i.e. at $\lambda_B = 0.1\sigma$, there occurs a quite different behavior. The collapsed regime disappears and we find a weak dependence of the brush height on anchoring density. In this case the counterion correlation is less pronounced as one can realize intuitively from a simulation snapshot shown in Fig. 5. The weak dependence of brush height on anchoring density is possibly a result of the repulsive Lennard-Jones interaction which is present in our finite simulation system. On the other hand, the osmotic regime is solely governed by the balance between the osmotic pressure of the counterions and the restoring force caused by the stretching energy of the chains.
Note that the third case shown in Fig. 3, i.e. small counterions, accidentally exhibits the same scaling law as the weak-coupling case. Nonetheless, the physical nature of these two regimes is quite different.

3.2 Partially Charged Chains

Simulations on partially charged polyelectrolyte brushes show quite different behavior for decreasing degree of charging f. In Fig. 6 brush heights versus anchoring densities are shown for the total range of charging $0 \leq f \leq 1$. On the one hand, at $f = 0$, we have the well known limit of a neutral brush $< z_m > \sim \rho_a^{1/3}$, on the other hand, at $f = 1$, we have the limiting scaling laws discussed above. At weak Coulomb coupling we find at any grafting density a monotonous stretching of the brush with increasing degree of charging. At strong interaction (left-hand side in Fig. 6) similar stretching is only found at dense

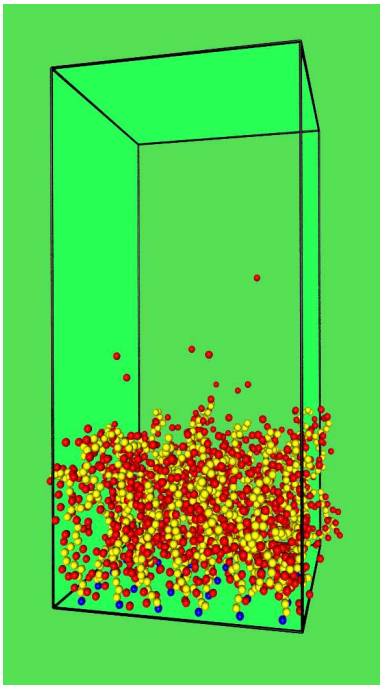

Figure 5. Simulation snapshot of a completely charged brush (36 chains of length 30) at weak Coulomb coupling $\lambda_B = 0.1\sigma$ and loose grafting density $\rho_a = 0.042\sigma^{-2}$.

grafting. For loose grafting densities, we observe a pronounced shrinking of the brush with increasing f. In the following section we will discuss how this unusual behavior can be understood on the basis of an extended scaling theory.

4 Comparison to Extended Scaling Theory

Recently a number of theoretical and numerical results have stressed the possibility of polyelectrolyte chain collapse at high charge densities. Let us use the simplest description which is able to produce these effects in a qualitative manner. In the bulk and in the low-density limit, the Debye-Hückel free energy density per unit volume is given by

$$f_{\mathrm{DH}}/k_{\mathrm{B}}T = -\frac{\kappa_D^3}{12\pi} \tag{5}$$

with the Debye length κ_D^{-1} for salt solutions of concentration c_s defined by $\kappa_D^2 = 8\pi\lambda_B c_s$. For low enough ion densities the Debye-Hückel approximation is a well-controlled approximation. More sophisticated approaches for treating the Coulomb correlations in simple electrolytes and polyelectrolytes (including the effect of the chain connectivity) lead to the same leading term given in Eq. (5).
Including the Debye-Hückel contribution F_{DH} the total free energy for a polyelectrolyte

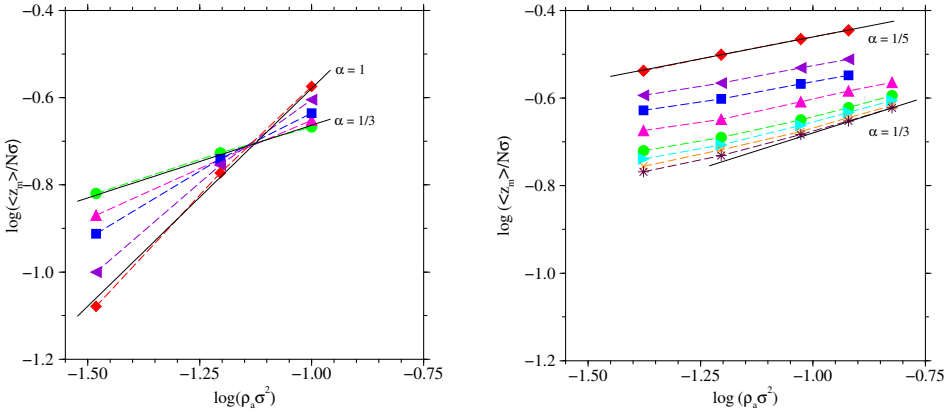

Figure 6. Average brush height (rescaled with the chains length N) versus anchoring density at different degree of charging, varying between $f = 1$ (red diamonds) and $f = 0$ (black stars). The limiting scaling laws are given as thin solid lines. Left-hand side: $\lambda_B = 0.7\sigma$, right-hand side: $\lambda_B = 0.1\sigma$. Because in the strong coupling case (left-hand side) the brush heights remain almost unchanged at small f, the smallest degree of charging plotted in this part of the figure is $f = 0.08$ (green circles).

brush in a good solvent becomes

$$F = F_{\rm st} + F_{\rm v2} + F_{\rm os} + F_{\rm electrost} + F_{\rm DH}, \tag{6}$$

where $F_{\rm st}$ is the stretching energy of the chains and $F_{\rm v2}$ the second virial (excluded volume) contribution. $F_{\rm os}$ stands for the osmotic free energy associated with the entropy costs for confining the counterions inside the brush and $F_{\rm electrost}$ is the direct electrostatic contribution occurring if counterions leave the brush which results in a violation of the local electro-neutrality.

Analyzing the total free energy Eq. (6), in addition to the previously known polyelectrolyte brush regimes we found that the Debye-Hückel correlation term induces a new collapsed brush regime (CB). Balancing the attractive interaction by the second virial the corresponding brush height becomes[10]

$$h_{CB} \sim N\rho_a v_2^2 f^{-3}\lambda_B^{-3}. \tag{7}$$

Note first that the scaling $h_{CB} \sim N\rho_a$, which results in a constant particle density inside the brush, is in agreement with the simulation results discussed above. Secondly we emphasize that Eq. (7) contains an additional scaling $h_{CB} \sim f^{-3}$. Such a shrinking of the brush with increasing f is in agreement with the behavior we have discussed above for strong coupling and loose grafting density. Thirdly, it should be noted that the second virial coefficient v_2 is an effective parameter. There is also an electrostatic contribution to v_2 which is repulsive for large ionic radii, but becomes negative for small ions.

The phase diagram in the $(f,\ \rho_a)$-space following from the total free energy Eq. (6) is shown in Fig. 7[10]. Clearly, in the weak coupling limit, i.e. at $\lambda_B < v_2^{1/3}$, we get the diagram of states previously obtained by Borisov et al.[11]. On the other hand, at strong coupling and strong charging, i.e. at $(v_2/\lambda_B^3)^{1/2} < f < 1$ the brush can undergo a first-order phase

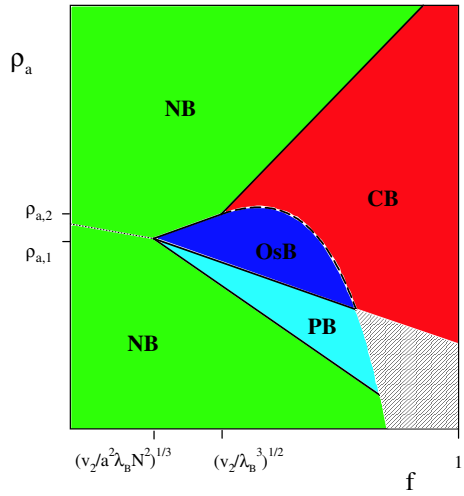

Figure 7. Scaling theory phase diagram for the polyelectrolyte brush on logarithmic scales at $(v_2/\lambda_B^3)^{1/2} < 1$. The different scaling regimes are the quasi-neutral regime (NB), the osmotic brush (OsB), the collapsed brush (CB) and the Pincus brush (PB). Solid lines indicate a crossover between different scaling regimes. The first order phase transition between OsB and CB regimes is shown by a (thick) dashed line. The thinly dashed line indicates the transition between strong and weak charging within the NB regime. The dashed region gives a crude estimation of the region where the simple scaling approach can not be applied.

transition from the osmotic into the collapsed state. Thus, the disappearance of the collapsed regime at small Bjerrum lengths, obtained in the simulations, is in agreement with the predictions of the theory. A qualitative understanding of the behavior at $\lambda_B = 0.7\sigma$ shown in the left-hand side of Fig. 6 can be obtained if one assumes a crossing of the CB - NB transition line in the upper part of the phase diagram Fig. 7 while reducing the degree of charging. Such an assumptions is reasonable, however, there is no way to succeed with a more quantitative picture. For the particular choice of simulation parameters, we have $\lambda_B^3/v_2 \approx 1$ which corresponds to the cross-over between strong and weak electrostatic coupling. In this case, the scaling theory allows no quantitative comparison with simulation results. However, it correctly describes the trends, namely that with increasing degree of charging f one goes to the collapsed brush regime.

5 Conclusion

In our simulation studies on polyelectrolyte brushes we found a novel collapsed brush regime not understood by theories known from literature. This fact stimulated the generalization of the theoretical picture. Now, the nature of the collapsed phase can be understood on the basis of a simple scaling model: Including in the total free energy a Debye-Hückel correlation term, indeed a new collapsed regime is obtained where the attractive Debye-Hückel interaction is balanced by the second virial of monomers and counterions.

The accessible region of the diagram of states is very sensitively dependent on the choice of parameters, in particular on the relation between Bjerrum length λ_B and second virial coefficient v_2. At this point we remind that in experiments on polyelectrolyte brushes no collapsed behavior has been reported so far, but the osmotic regime seems dominating[7]. On the other hand, up to now no osmotic behavior has been seen in simulations, but brush collapse appears to be a major feature if Bjerrum length and second virial coefficient are straightforwardly chosen as 'bare' parameters. For obvious reasons this observation suggests that with such a choice of the simulation parameters we are studying the strong coupling case. Indeed, reducing the Bjerrum length at fixed second virial coefficient, considerable stretching of the polyelectrolyte brush together with a weak dependence on grafting density is obtained. Thus, to bridge the gap between simulation and experiment more insight is necessary in order to be able to chose appropriate and well-founded parameters.

Acknowledgements

The work was supported by the Deutsche Forschungsgemeinschaft within the Schwerpunktprogramm Polyelektrolyte. We gratefully acknowledge grants of computer time provided by NIC Jülich and ZIB Berlin.

References

1. D. H. Napper, *Polymeric Stabilization of Colloidal Dispersions* (Academic Press, New York, 1983).
2. P. Pincus, *Colloid Stabilization with Grafted Polyelectrolytes*, Macromolecules **24**, 2912–2919 (1991).
3. J. Lekner, *Summation of Coulomb Fields in Computer-Simulated Disordered Systems*, Physica A **176**, 485–498 (1991), R. Sperb, *Extension and Simple Proof of Lekner's Summation Formula for Coulomb Forces*, Mol. Simulation **13**, 189–193 (1994).
4. G. S. Grest and K. Kremer, *Molecular Dynamics Simulation for Polymers in the Presence of a Heat Bath*, Phys. Rev A **33**, 3628–3631 (1986).
5. M. P. Allen and D. J. Tildesley, *Computer Simulation of Liquids* (Oxford University Press, Oxford, 1987).
6. W. Gropp, E. Lusk and A. Skjellum, *Using MPI* (The MIT Press, Cambridge, MA, 1994).
7. H. Ahrens, S. Förster and C. A. Helm, *Polyelectrolyte Brushes Grafted at the Air/Water Interface*, Macromolecules **30**, 8447–8452 (1997); *Charged Polymer Brushes: Counterion Incorporation and Scaling Relations*, Phys. Rev. Lett. **81**, 4172–4175 (1998).
8. F. S. Csajka and C. Seidel, *Strongly Charged Polyelectrolyte Brushes: A Molecular Dynamics Study*, Macromolecules **33**, 2728–2739 (2000).
9. H. Schiessel and P. Pincus, *Counterion-Condensation-Induced Collapse of Highly Charged Polyelectrolytes*, Macromolecules **31**, 7953–7959 (1998).
10. F. S. Csajka, R. R. Netz, C. Seidel and J.-F. Joanny, *Collapse of Polyelectrolyte Brushes: Scaling Theory and Simulations*, Eur. Phys. J. E **4**, 505–513 (2001).
11. O. V. Borisov, E. B. Zhulina and T. M. Birstein, *Diagram of States of a Grafted Polyelectrolyte Layer*, Macromolecules **27**, 4795–4803 (1994).